JOURNAL OF THERMOPHYSICS AND HEAT TRANSFER
Vol. 10, No. 3, July–September 1996

Determining Electron Temperature and Density in a Hydrogen Microwave Plasma

Carl D. Scott*
NASA Johnson Space Center, Houston, Texas 77058
Samir Farhat,† Alix Gicquel,‡ and Khaled Hassouni§
Université Paris Nord, 93430 Villetaneuse, France
and
Michel Lefebvre¶
Office National d'Etudes et de Recherches Aérospatiales, B. P. 72, 92322 Châtillon, France

A three-temperature thermochemical model is developed for analyzing the chemical composition and energy states of a hydrogen microwave plasma used for studying diamond deposition. Chemical and energy exchange rate coefficients are determined from cross-sectional data, assuming Maxwellian velocity distributions for electrons and heavy species. These coefficients are then used to solve a zero-dimensional problem for the species mole fractions and the electron and vibrational temperatures using measured rotational temperatures. The calculations are made for three cases in which the size of the plasma is held fixed while varying the microwave power and the pressure. The vibrational temperature results agree well with a case in which the vibrational temperature was measured using coherent anti-Stokes Raman spectroscopy. The vibrational temperature is shown to approach the translational temperature as the pressure and power are increased. The H-atom mole fraction increases significantly with power and pressure, whereas the ion fraction and the electron temperature tend to decrease. The calculated H-atom fractions compare well with measured values.

Introduction

HYDROGEN plasmas with a few percent of methane have been used to produce diamond films in the laboratory. The rates of deposition and etching of graphite and diamond on substrates are significantly affected by the concentrations of the various species and the energy states in which they exist. Likewise, the surface temperature and flow pattern in the reactor affect transport of reactive species to the surface. A research program with the objective of determining the chemistry, flowfield, and energy states of a hydrogen microwave plasma is underway to help understand how to optimize diamond deposition. Eventually, the flow simulation must include the carbon-containing species, but here the analysis concerns a pure hydrogen plasma. Measurements of the vibrational and rotational energy modes, and H-atom molar fraction via optical emission spectroscopy, two-photon-allowed transition laser-induced fluorescence (TALIF), and coherent anti-Stokes Raman spectroscopy (CARS) are useful to validate the model, and the model may be used to infer properties not measured, particularly, species mole fractions, the electron density, and electron and vibrational temperatures.

Received Dec. 16, 1993; revision received Jan. 23, 1996; accepted for publication Jan. 30, 1996.

*Senior Research Engineer, ES3. Associate Fellow AIAA.
†Maitre de Conference, Laboratoire d'Ingéniérie des Matériaux et des Hautes Pressions.
‡Professor, Laboratoire d'Ingéniérie des Matériaux et des Hautes Pressions.
§Research Associate, Laboratoire d'Ingéniérie des Matériaux et des Hautes Pressions.
¶Research Engineer.

A nonequilibrium energy exchange and chemical reaction model was developed[1] for use in a computational fluid dynamics calculation for a hydrogen plasma excited by microwaves. The model takes into account the energy exchange between the electrons and molecular and atomic hydrogen. Specifically, electron–translation, electron–vibration, translation–vibration, ionization and dissociation are included. The model assumes three temperatures: 1) translational/rotational, 2) vibrational, and 3) electron, each describing a Maxwell/Boltzmann distribution for its respective energy mode. In that model the energy from the microwave source is coupled to the energy equation via a source term that depends on an effective electric field. The electric field, or more specifically, the energy absorbed from the field, is estimated from the radiated microwave power and compared with the energy lost by electrons via collision processes involving the atoms and molecules.[2] However, to find the electric field one would have to solve Maxwell's electrodynamics equations, coupled with the fluid equations. In this model, knowledge of the exact value of the electric field is not necessary since the absorption of the electrical energy appears in the microwave power density term. An average value of the latter may be estimated from the ratio of total input power and the plasma volume. The subject of modeling the energy exchange between the various energy states in hydrogen plasmas has been developed over the last two or three decades with various degrees of complexity, depending on the plasma conditions. Cross sections and reactions rates for electron–hydrogen collisions have been measured and calculated by a number of workers. These interactions involve dissociation, excitation, electron–vibration energy exchange, ionization and translational–vibrational energy exchange, as well as chemical reactions involving neutral and ionized species. The various paths of energy loss from electrons to the internal degrees of freedom of hydrogen and to the translational/rotational degrees of freedom affect the ultimate conditions of the plasma and the possible chemical reactions both in the gas phase and on surfaces.

The model is developed for specific plasma conditions for a diamond deposition reactor. A pressure level of from 2.5 to 10 kPa has been established to assure a reasonable rate of deposition. The plasma is established by a microwave system operating from about 600 to 2000 W. A schematic of the apparatus is given in Fig. 1. An approximately hemispherical active plasma zone exists next to the substrate surface, which forms a boundary of the plasma. The extent and conditions of the plasma depend on the power coupled to this cavity as well as the electron and energy loss mechanisms in the plasma. These loss mechanisms include diffusion of electrons and excited species to the surface and out of the active zone, electron energy loss by collision with H_2 to form vibrationally or electronically excited molecules, dissociation of the molecules, ionization of atoms and molecules, and electron–translation/rotation exchange. Forced and free convection may also play a role in loss of electrons and other excited species from the plasma zone by removing them from the active plasma zone, but these are neglected in this study. Also neglected are losses at the almost hemispherical gaseous boundary of the active zone.

Modeling of hydrogen plasmas and the study of energy exchange mechanisms have been done by several workers in other applications. Among them are the works of Gorse et al.,[3,4] who applied their models to multicusp magnetic discharge plasma, and Loureiro and Ferreira,[5] who applied their model to the positive column of a dc discharge. These applications are at sufficiently low temperature and pressure, so that it was unquestionably necessary to account for the strong nonequilibrium associated with the electronic energy distribution function (EEDF). Their distributions were expected to deviate from a Maxwell/Boltzmann distribution. A model for a higher-pressure hydrogen plasma was proposed by Koemtzopoulos et al.[6] for their axisymmetric flow tube reactor. Their model accounted for a non-Maxwellian EEDF by solving the Boltzmann equation. However, they did not consider a separate vibrational temperature, although they did account for transfer of energy between electrons and vibration. They found that their EEDF did deviate from a Maxwellian, even at relatively high pressures, and had an essentially bimodal behavior. The distribution function at high electron energy could be characterized by a lower temperature than in the low-energy range, as was seen by a change in slope in their EEDF Boltzmann plot. (They might have obtained the opposite behavior if they had accounted for superelastic collisions.) In the present case we have not solved the Boltzmann equation, but have assumed that the distribution functions are Maxwell/Boltzmann, even though the pressure and temperature may not be sufficiently high for the electron energy distribution function to be actually Maxwellian, and the vibrational distribution function of H_2 to be actually Boltzmann. However, the temperatures describing these Maxwell/Boltzmann distributions for the various degrees of freedom are assumed not to be the same, nor are they equal to the translational/rotational temperature. In this study it will be seen that one may obtain the electron density by measuring the vibrational temperature and employing the equations that couple the energy modes. CARS measurements[7] show that the vibrational temperature is slightly above (100–200 K) the rotational temperature throughout the plasma for the 2500 Pa case. CARS measurements were not made for the other two cases discussed in this article.

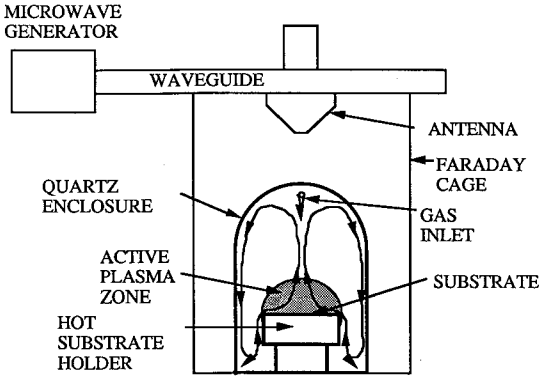

Fig. 1 Schematic of hydrogen microwave plasma diamond deposition apparatus.

Zero-Dimensional Model Equations with Diffusion Correction

The general nonequilibrium three-temperature model[1] for the hydrogen microwave plasma was developed in full three-dimensional time-dependent flow of arbitrary speed. The model is reduced to essentially zero dimension in chemistry and vibrational energy, but we account for the loss of ions and atoms on the surface by an approximate diffusion loss term. By assuming zero bulk velocity the flow equations can be written as follows for the species and energy equations:

$$\frac{dc_s}{dt} = \omega_s - \xi_s \tag{1}$$

The energy equations are reduced by eliminating the convection and diffusion terms. The following zero-dimensional energy equations for electron, vibration, and total energy are relaxed to steady state:

$$\frac{de_e}{dt} = -Q^e_{ex} + \sigma E^2 \tag{2}$$

$$\frac{de_v}{dt} = Q^v_{ex} - \text{boundary losses} \tag{3}$$

$$\frac{de_{Tot}}{dt} = -Q_{rad} + \sigma E^2 - \text{boundary losses} \tag{4}$$

The left-hand side of energy Eqs. (2–4) are the energy exchange and source terms to be defined subsequently. Equation (4) is given for completeness, but is not used in further analysis because we have eliminated it by use of a measured gas temperature. The boundary loss term in Eq. (3) is neglected in further analysis because it is small and because the vibrational energy accommodation at a surface is not known.

The power per unit volume absorbed from the microwave electromagnetic field is $Q_{mw} = \sigma E^2$, where σ is the electrical conductivity of the plasma and E is the electric field. Energy exchange between the electrons, vibration, translation/rotation, and dissociation is accounted for. Q_{rad} is the energy loss term associated with molecular and atomic radiation. The rate of exchange of energy per unit volume between various modes of energy and vibration is

$$\frac{de_v}{dt} = Q^v_{ex} = Q_{Tv} + Q^{1v}_{ev} + Q_{ev} \tag{5}$$

where Q_{Tv} is for exchange between vibration and translation of molecules and atoms, Q_{ev} is for the direct exchange between electrons and vibrational states in the ground electronic state, and Q^{1v}_{ev} is the vibrational excitation of ground state H_2 by electrons via excitation to singlet electronic states that then radiate, leaving the molecule in vibrationally excited ground electronic states.

The net electron energy equation (losses of energy by electrons are positive here), is

$$\frac{de_e}{dt} = Q^e_{ex} = Q_{mw} - (Q_{Te} + Q_{ev} + Q^{1e}_{ev} + Q^3_{ed} + Q_{ei}) \tag{6}$$

where $Q_{mw} = \sigma E^2$ is the absorbed microwave power per unit volume, Q_{Te} is translation–electron exchange energy, Q_{ed}^3 is the energy lost by electrons because of the dissociation via excitation of triplet states, and Q_{ei} is the energy lost by ionization of H_2 and H. We could neglect Q_{ev}^{1v} because it is small for the conditions considered, but Q_{ev}^{1e} is a significant loss term for the electrons. The difference in power loss $Q_{ev}^{1e} - Q_{ev}^{1v}$ is accounted for by molecular radiation. There is another molecular radiative loss caused by the excitation of the b and c triplet states, which radiate to the a triplet state before the H_2 molecule dissociates. The electron temperature is obtained from the expression for the internal energy per unit volume $e_e = \frac{3}{2} n_e k T_e$. Since the gas temperature is a measured quantity in this study, we will not hereafter address the total energy Eq. (4) in which the radiative loss Q_{rad} appears. Also, under the assumption that all energy modes are Maxwell/Boltzmann, we do not need to keep track of populations of the excited states produced by chemical reactions.

Electron–Vibration Exchange

There are two paths to vibrational exchange with electrons. The first is direct vibration excitation and de-excitation in a given electronic state, in particular, the ground state. The second is vibrational excitation via electronic excitation of excited electronic singlet states followed subsequently by a radiative transition to a vibrationally excited ground state. Cross sections for these reactions are given by Buckman and Phelps.[8,9]

Direct Ground Electronic State Excitation of $H_2(v)$

The rate coefficients in cm^3/s/atom for these reactions are calculated by integrating the cross sections over the Maxwellian electron energy distribution function

$$k_{0j}(T_e) = 6.70 \times 10^7 T_e^{-3/2} \int_{E_0}^{\infty} \sigma_{0j}(E) E \exp\left(-\frac{E}{T_e}\right) dE \quad (7)$$

where the energy E and the temperature are in electron–volts. E_0 is the threshold energy of the exchange, and cross section σ_{0j} is in cm^2.

The relaxation time τ_{ev} is determined following the procedure developed in the appendix of Lee's[10] article:

$$\tau_{ev} = \frac{1}{n_e[1 - \exp(-\theta_v/T_e)]^2 \frac{1}{2} \int k_{0j} j^2 \, dj} \quad (8)$$

It has been assumed that the vibrational levels are closely spaced so that the integral in Eq. (8) well represents a sum over levels. This may not be the case for H_2, but we will use it until the error is determined to be too large. The form of k_{0j} for the first three vibrational levels (j = 1–3) are very similar in shape. Therefore, an approximation was made that the integral in Eq. (8) could be done semianalytically by fitting the maxima of the k_{0j} to a simple function of the form:

$$k_{0j}^{max} = 3.39 \times 10^{-8} e^{-2.401j} \quad (9)$$

which can be integrated analytically. The peak values are shown in Fig. 2. A polynomial curve fit of the result is shown in the figure. The relative rate coefficient function was integrated numerically to obtain a constant factor. The resulting relaxation time τ_{ev} as a function of electron energy is given in Fig. 3. The loss rate of energy is obtained from the relaxation time by the relation:

$$Q_{eV} = \rho_{H_2} \frac{de_v}{dt} = \rho_{H_2} \frac{e_v^{**}(T_e) - e_v}{\tau_{ev}} \quad (10)$$

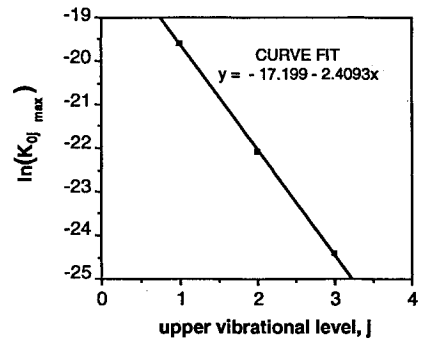

Fig. 2 Curve fit of peak values of electron–H_2–vibration rate coefficients.

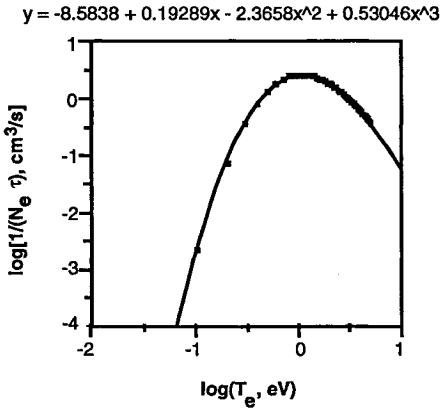

Fig. 3 Curve fit of electron-H_2-vibration relaxation time based on cross sections.

where $e_v^{**}(T_e)$ is the equilibrium vibrational energy evaluated at the electron temperature (the driving energy), and e_v is the vibrational energy per unit mass to be determined.

Vibrational Excitation of $H_2(v)$ via Excitation of H_2 Singlets

Electrons may excite the $B^1\Sigma$ and $C^1\Pi$ states that then radiate to the $H_2(X, v)$ ground electronic state. It requires about 10.5 eV to excite the singlets, but the molecules end up with only about 1 eV in vibration. Thus, there is a large electron energy loss, but only a modest gain of vibrational energy. The balance of the energy is lost from the plasma via radiation. The rate coefficients may be calculated from total cross sections of Buckman and Phelps[8,9] with the probabilities for specific vibrational states obtained from Hiskes,[11] who has calculated F(B, v, v'') and F(C, v, v''), the probabilities of exciting an $X^1\Sigma(v'')$ state from an $X^1\Sigma(v)$ state via excitations of the $B^1\Sigma$ and $C^1\Pi$ states, respectively. We have used these probabilities to compute the energy transferred from electrons to vibration using the relation:

$$Q_{ev}^{1v} = n_{H_2} R \theta_v [k_{ev}^{B1}(T_e) S_B(T_v) + k_{ev}^{C1}(T_e) S_C(T_v)] \quad (11)$$

where

$$S_B(T_v) = \sum_{v=0}^{14} \exp(-E_v/RT_v)/Z_v(T_v) \sum_{v''=0}^{14} F(B, v, v'')(\varepsilon_v - \varepsilon_v'') \quad (12)$$

$$S_C(T_v) = \sum_{v=0}^{14} \exp(-E_v/RT_v)/Z_v(T_v) \sum_{v''=0}^{14} F(C, v, v'')(\varepsilon_v - \varepsilon_v'') \quad (13)$$

where $\varepsilon_v = E_v/R\theta_v$ is the dimensionless vibrational energy of level v; and $k_{ev}^{B1}(T_e)$ and $k_{ev}^{C1}(T_e)$ are the rate coefficients for

Table 1 Energy exchange rate formulas and constants

Interaction formula	Constants, a_i			
	a_0	a_1	a_2	a_3
Singlet electron/vibration, $500 < T_v < 4700$ K				
$S_B(T_v) = \Sigma_{i=0}^{2} a_i T_v^i$	3.2179	1.9571e-5	−1.4701e-8	——
$S_C(T_v) = \Sigma_{i=0}^{2} a_i T_v^i$	3.3031	−2.0333e-6	−2.4737e-8	——
Arrhenius,[a] $0.1 < T_e < 5.0$ eV				
$k_{ev}^{B1}(T_e)$, cm³/s/mol	9.441e-9	0	133,270 K	——
$\varepsilon_B = 1.776 \times 10^{-18}$ J/mol				
$k_{ev}^{C1}(T_e)$, cm³/s/mol	1.0563e-8	0	150,900 K	——
$\varepsilon_C = 1.952 \times 10^{-18}$ J/mol				
Direct electron/vibration,[a] $0.1 < T_e < 5.0$ eV	−9.7748	0.0073464	−2.2301	0.54929
$\log(1/n_e\tau_{ev}) = \Sigma_{i=0}^{3} a_i[\log(T_e, \text{eV})]^i$, cm³/s/mol				
Vibration–translation, ($H + H_2$[b] $\rightarrow H + H_2$) quenching,[c]				
k_{10}, cm³/s/mol, Arrhenius				
Reactive, $300 < T < 4000$ K	7.682e-11	0	2192 K	——
Nonreactive, $300 < T < 4000$ K	3.707e-11	0	2140 K	——
Vibration–translation (H_2),[b] atm-s	$p\tau_{H_2\text{-}H_2} = 3.9 \times 10^{-10} \exp(-100/T^{1/3})$		——	——

[a]Calculated from cross sections in Buckman and Phelps.[9] [b]Kiefer and Lutz.[16] [c]Gorse et al.[4]

electron excitation of the singlets calculated from the total cross sections. These cross sections could have been taken to be equal as indicated by Hiskes[11]; however, here they were calculated individually from the cross sections given in Ref. 9. Curve fits of the results are given in Table 1. The initial ground vibrational quantum number is v and the final one is v''. Here, the term $\exp(-E_v/RT_v)/Z_v(T_v)$ is the weighting factor for the number of H_2 molecules in state v, and $Z_v(T_v)$ is the vibrational partition function. The factors $S(T_v)$ were evaluated as functions of T_v and were then curve fit using third-degree polynomials. The results are given in Table 1. The vibrational energy levels are calculated from the spectroscopic constants $\omega_e = 4401.21$ cm^{-1} and $\omega_e\chi_e = 121.336$ cm^{-1}. The S functions are
calculated assuming anharmonic oscillator energy levels given by

$$E_v = hc[\omega_e(v + \tfrac{1}{2}) - \omega_e\chi_e(v + \tfrac{1}{2})^2] \tag{14}$$

Electron Energy Loss by Excitation of Singlet H_2 States

The loss of energy by electrons in exciting the singlet states of H_2 is given by the rate of excitation of those states times the energy lost per excitation ε:

$$Q_{ev}^{1e} = n_e n_{H_2}(k_{ev}^{B1}\varepsilon_B + k_{ev}^{C1}\varepsilon_C) \tag{15}$$

Translation–Vibration Relaxation with Molecules and Atoms

One could calculate the T–v exchange for molecules by summing over all rate probabilities as shown in Ref. 12, and basing the rates on the data of Billing and Fisher[13] and the method of Audibert et al.[14] This requires keeping track of the population of all vibrational states. Instead, in keeping with the assumption of Boltzmann distributions, we shall adopt some of the modeling methods of Lee,[10] who applied Landau–Teller-type relations for vibration–translation relaxation to mixtures of nitrogen and oxygen. The energy exchange rate is given by

$$Q_{Tv} = \rho_{H_2}\frac{e_v^*(T) - e_v}{\tau_{v_{H_2}}} + \rho_{H_2}\frac{e_v^*(T) - e_v}{\tau_{v_H}} \tag{16}$$

where $e_v^*(T)$ is the specific vibrational energy at the translational temperature, e_v is the vibrational energy of the flow, and τ_{v_H} is the relaxation time for T–v relaxation caused by collisions of H_2 with H, and $\tau_{v_{H_2}}$ is the relaxation time for collisions of H_2 with H_2. Lee[10] has given the general form for relaxation of molecular species 1 in a mixture:

$$\tau_{vl} = \sum_{i \neq e^-} X_i \Big/ \sum_{i \neq e^-} \frac{X_i}{\tau_{v_{li}}} \tag{17}$$

The $\tau_{v_{H_2}}$ values can be determined from either the Millikan and White[15] or Kiefer and Lutz[16] correlations. Audibert et al.[13] have shown that the Kiefer and Lutz correlations agree with their higher temperature results over a fairly broad temperature range of interest here. The Kiefer and Lutz correlation, which we have used in the present calculations, is

$$\tau_{v_{H_2H_2}}p = 3.9 \times 10^{-10} \exp(100/\sqrt[3]{T}) \text{ atm-s} \tag{18}$$

The relaxation scheme for atoms exchanging translational energy with molecules involves significant quenching of hydrogen molecule vibrational states. The rates are given in the appendix of Gorse et al.,[4] and we have determined $\tau_{v_{H_2H}}$ in a similar fashion to that for electron–vibration exchange. In particular, the relaxation time was based on the rate k_{01} for excitation of $H_2(v = 0)$ to $H_2(v = 1)$, considering both reactive and nonreactive collisions. Gorse et al.[4] obtained the rate coefficients in Arrhenius form by a curve fit from which the relaxation time was derived. The curve fit coefficients are given in Table 1. The relaxation times are obtained from the rate coefficients using

$$n_H\tau_{v_{H_2H}} = 1/(k_{10}^{nr} + k_{10}^{r})$$

where the explicit vibrational excitation by collisions with atoms does not appear.

Chemical Reaction Model

There are at least 27 chemical reactions that describe the chemical kinetics of a nonequilibrium plasma at conditions associated with the present experiments. They fall into two basic categories. First are those that involve reactions with electrons, e.g., dissociation and ionization, while the other category includes heavy particles, including charge exchange and recombination of ions and atoms. This complete set of reactions is given in Table 2, along with their corresponding rate coefficients. This set of chemical reactions is written in general forward form as

$$\sum_i \nu_{ir}' A_i \rightarrow \sum_i \nu_{ir}'' A_i \tag{19}$$

Table 2 Reactions and rate constants for a moderate pressure hydrogen plasma

Reaction	Constants, $k = AT^{\eta e^{-T_a/T}}$ A, cm³/s/mole	η	T_a, K	Temperature range	Governing temperature	Source of data
$e + H_2(v) \rightarrow e + H_2^+ + e$	1.18×10^{16}	0	191,500	$<10^4$–5×10^4 K	T_e[a]	From cross sections[9]
$e + H \rightarrow e + H^+ + e$	1.08×10^{16}	0	178,210	1–6 eV	T_e	From cross sections[28]
$e + H_2(v) \rightarrow e + H_2^* \rightarrow e + 2H$	1.2×10^{16}	0	113,500	$<10^4$–5×10^4 K	T_e[a]	From cross sections[9]
$e + H_3^+ \rightarrow 3H$	8.0×10^{17}	−0.404	0	0.1–1 eV	T_e	Janev[19] from cross sections 2.2.15a,b
$e + H_3^+ \rightarrow H_2^*(v > 5) + H^*(n = 2)$	3.2×10^{17} 2.5:1					
$e + H_3^+ \rightarrow e + H^+ + 2H$	1.22×10^{17}	0	179,380	5,000–50,000 K	T_e	Janev[19] from curve fit 2.2.16
$e + H_2(v) \rightarrow H + H^-(v \geq 4)$[b]	2.24×10^{22}	−1.45	9,592	5,000–50,000 K	T_e, T_v	Janev[19] 2.2.17
$e + H_2^+ \rightarrow e + H^+ + H$	1.46×10^{17}	0	37,460	5,000–50,000 K	T_e	Janev[19] 2.2.12
$e + H_2^+ \rightarrow H + H^*(n)$	9.44×10^{18}	−0.604	0	5,000–50,000 K	T_e	Janev[19] 2.2.14
$2e + H^+ \rightarrow e + H$	3.63×10^{37} cm⁶/s/mole²	−4.0	0	300–5,500 K	T_e	Johnson and Hinnov[22,23]
$e + H^- \rightarrow 2e + H$	1.34×10^{13}	0.9	22,700	5,000–50,000 K	T_e	Janev[19] 7.1.1
$e + H^+ \rightarrow h\nu + H$	1.46×10^{14}	−0.699	0	250–64,000 K	T_e	Massey[21]
$2H + H_2 \rightarrow H_2 + H_2$	1.0×10^{17} cm⁶/s/mole²	−0.6	0	50–5,000 K	T	Cohen and Westburg[29]
$2H + H \rightarrow H_2 + H$	3.2×10^{15} cm⁶/s/mole²	0	0	50–5,000 K	T	Cohen and Westburg[29]
$H_2^+ + H \rightarrow H^+ + H_2$	3.85×10^{14}	0	0	——	T	Karpas et al.[30]
$H_2^+ + H_2 \rightarrow H_3^+ + H$	1.27×10^{15}	0	0	——	T	Karpas et al.[30]
$H_2 + H_2 \rightarrow H + H + H_2$	8.61×10^{17}	−0.7	52,530	600–5,000 K	T[a]	Cohen and Westburg[29]
$H_2 + H \rightarrow H + H + H$	2.7×10^{16}	−0.1	52,530	600–5,000 K	T[a]	Cohen and Westburg[29]
$H + H^- \rightarrow e + 2H$	4.5×10^8	1.5	698	1,100–11,000 K	T	Janev[19] 7.3.2a
$H + H^- \rightarrow e + H_2^*(v)$	1.43×10^{15}	−0.146	815	1,100–11,000 K	T	Janev[19] 7.3.2b
$H^+ + H_2 \rightarrow H + H_2^+$	1.90×10^{14}	0	21,902	1,100–11,000 K	T	Phelps[31]
$H^+ + H^- \rightarrow H^*(n = 3) + H(1s)$	1.78×10^{17}	0	1,768	1,100–11,000 K	T	Janev[19] 7.2.3
$2e + H_2^+ \rightarrow \varepsilon + 2H$	3.17×10^{21}	−4.5	0	——	T_e	Raizer[32]
$2e + H_3^+ \rightarrow \varepsilon + H + H_2$	3.17×10^{21}	−4.5	0	——	T_e	Raizer[32]
$H^+ + 2H_2 \rightarrow H_3^+ + H_2$	1.95×10^{20}	−0.5	0	——	T	Matveyev and Silakov[33]
$H^- + H_2^+ \rightarrow H_2 + H$	2.08×10^{18}	−0.5	0	——	T	Matveyev and Silakov[33]
$H^- + H_3^+ \rightarrow H_2 + H_2$	2.08×10^{18}	−0.5	0	——	T	Matveyev and Silakov[33]

[a]The reactions involving H_2 actually depend on T_v as well as T, but cross section data that depends on vibrational excitation states are not available.
[b]Rate must be reduced by Boltzmann factor for $v \geq 4$.

where ν'_{ir} and ν''_{ir} are the stoichiometric coefficients for species A_i. Reverse reactions are written explicitly as forward reactions. Thus, the general species production rates are written

$$\omega_i = \sum_r (\nu''_{ir} - \nu'_{ir}) k_{fr} \prod c_i^{\nu'_{ir}} \tag{20}$$

where k_{fr} is the rate coefficient for the rth reaction. The net rate of molar production of species i is

$$\frac{dc_i}{dt} = \omega_i - \xi_i \tag{21}$$

where c_i is the concentration of species i, ω_i is the rate of volume production, ξ_i is the rate of (loss) at the wall, and n_s is the number of species considered in the plasma.

The loss rate of ions and atoms at the wall is calculated from the kinetic flux that is set equal to the diffusive flux. The wall loss rate is given by

$$\xi_i = \frac{S_w}{V_p} \sum_r \mu_{ir} c_i^w k_r \tag{22}$$

where c_i^w is the wall concentration of species i, μ_{ir} is the stoichiometric coefficient, k_r is the reaction rate in cm/s, S_w is the area of the wall, and V_p is the volume of the plasma. If we assume the loss is from a hemispherical volume on a circular surface, both of radius R, then the surface to volume ratio is $3/2R$. To calculate the wall concentration in Eq. (22) we assume the equality between the loss flux at the surface given by kinetic theory and the diffusion flux calculated assuming a linear profile of concentration in the boundary layer of thickness δ_i. The flux according to kinetic theory is (assuming the Debye length is much smaller than all dimensions of interest so that we can ignore the Bohm criterion velocity)

$$N_i = c_i^w k_{ri} = c_i^w \gamma_r \sqrt{kT_w/2\pi m_i} \tag{23}$$

where γ_r is the probability of reaction r on the surface. Setting this expression for the flux equal to the diffusion flux

$$N_i = D_i \frac{dc_i}{dy} \approx D_i \frac{c_i^w - c_i}{\delta_i} \tag{24}$$

we can solve for the wall concentration c_i^w

$$c_i^w = c_i \frac{1}{1 + (k_{ri}\delta_i/D_i)} \tag{25}$$

D_i are the diffusion coefficients of species i with the mixture computed from cross sectional data of Yos,[17] using the relation of Curtiss and Hirschfelder.[18] The ion diffusion coefficients were corrected for the ambipolar field by using the factor $(1 + T_e/T)$. The set of reactions (21) may be relaxed to zero by a numerical technique.

The reaction rates for ionization of H_2 and H by electrons given in Table 2 are calculated from cross-sectional data from Refs. 8 and 9 by integration over the electron energy distribution function that is assumed to be Boltzmannian at an electron temperature T_e. A plot and curve fit of the ionization rate coefficient for H_2 are given in Fig. 4, where the cross sections were obtained from Refs. 8 and 9. Even though the conditions under which these cross sections were obtained may not correspond to a Maxwellian EEDF, we have assumed a Boltzmann distribution for the electrons here, and we have used the

cross sections of Ref. 9 directly. These rates are compared with rates computed from cross-sectional curve fits given by Janev et al.[19] and with rates computed from Janev et al. cross sections using a non-Maxwellian EEDF by Koemtzopoulos et al.[6] There is a wide difference in the rates, depending on which distribution function is used and depending on which source of cross-sectional data. It is believed that the Buckman and Phelps[9] cross sections are preferred because the curve fits of Janev et al. are not very good at low energies because of the fact that they fit the data over a very wide range of energies and that near threshold the cross section rises steeply with energy.

The rate of deionization is evaluated at the electron temperature T_e. The dominant ion has been estimated to be the H_3^+ ion, therefore, reactions involving production and depletion of H_3^+ are important for electron recombination. Electron detachment and dissociative attachment also contribute to the charge balance. H^+ is the other dominant positive ion. Recombination of hydrogen atomic ions can follow two paths, one is three-body recombination, whereas the other is radiative recombination as indicated in Table 2. The rate of three-body recombination depends on the energy level in which the H-atom is found, thus on the kinetics of the problem and the electron density and temperature. For sufficiently high electron temperature and low electron density the recombination coefficient is fairly insensitive to the electron density because it is dominated by radiative recombination. Radiation trapping of the Lyman-α line can affect the rate of recombination since the number density of the ground and excited states of the atoms may be affected. Drawin and Emard[20] have solved the master equations, taking into account both three-body recombination and radiative recombination with radiative absorption. Their results show a dependence on electron density in lower temperature and higher density regimes. Their results are shown in Fig. 5 along with the purely radiative recombination rate from Massey[21] and purely three-body recombination rate for relatively high electron density of Johnson and Hinnov,[22] who curve-fit measurements of Ref. 23. Both of these paths to H^+ recombination are slow for the conditions here.

Vibrational Energy Balance

The vibrational energy in the plasma at steady state is given by Eq. (3). At an imagined symmetry plane of a bounded plasma the vibrational energy is balanced when the $e-V$ exchange equals $T-V$ exchange because diffusion and conduction is zero there because of symmetry. Equation (5) becomes $Q_{ex}^v = 0$, or

$$\frac{e_v^*(T) - e_v(T_v)}{\tau_v} + \frac{e_v^{**}(T_e) - e_v(T_v)}{\tau_{ev}} + Q_{ev}^{1v} = 0 \qquad (26)$$

where

$$\tau_v = \frac{X_{H_2} + X_H}{(X_{H_2}/\tau_{v_{H_2H_2}}) + (X_H/\tau_{v_{H_2H}})}$$

and where $\tau_{v_{H_2}}$ and τ_{v_H} are translation–vibration relaxation times for $H_2(v)-H_2$ and $H_2(v)-H$ interactions, respectively, and τ_{ev} is the electron–vibration relaxation time. The asterisk (* and **) superscripts merely call attention to the fact that these functions are evaluated at the translational and electron temperature, respectively. We have assumed that only one molecule, H_2, contributes to the vibrational energy because its mole fraction is orders of magnitude greater than the other molecules in the system. For that reason we have dropped a subscript H_2 from the relaxation times and vibrational energy. Curve-fit coefficients for these relaxation times are found in Table 1. The vibrational energy e_v in J/kg is given by the relation for harmonic oscillators:

$$e_v(T) = (kN_a/W)\theta_v/[\exp(\theta_v/T) - 1] \qquad (27)$$

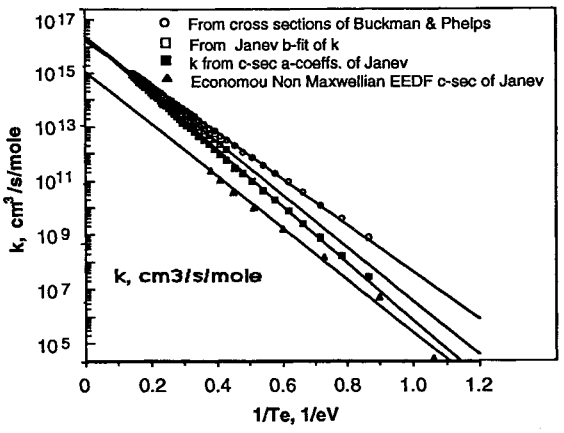

Fig. 4 Comparison of rate coefficients for ionization of H_2 by electrons: cross sections from Buckman and Phelps[9] and from Janev et al.[19] using Maxwellian EEDF and Economou non-Maxwellian EEDF.

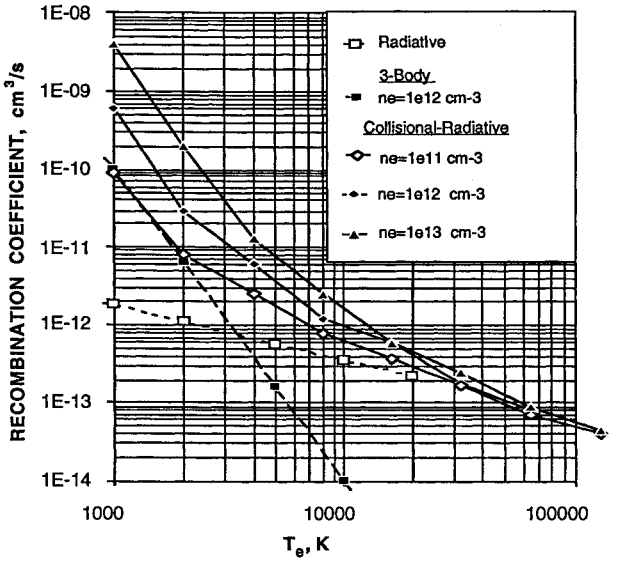

Fig. 5 Recombination rate for $H^+ + e$ in various T_e and n_e domains given by three-body, radiative, and collisional–radiative recombination paths.

The characteristic vibrational energy (first excited state) for hydrogen is $\theta_v = 5987$ K. Avagadro's number and molecular weight are N_a and w, respectively.

Maximum Power Coupled to the Plasma

The microwave antenna provides power that excites and maintains the plasma. Most of the microwave power that is radiated is absorbed by the plasma. If we assume that the energy is absorbed uniformly throughout the volume V of the visible plasma, then we can estimate the power absorbed by the electrons. This will put an approximate upper bound on the average absorbed power, limiting conditions in the plasma such as T_e and n_e. This condition is found where Q_{ex}^e equals the average absorbed microwave power P_{mw}/V. This condition leads to an electron energy balance [Eq. (6)] from which the electron temperature is determined, simultaneously with the vibrational energy balance Eq. (26) and the species rate Eqs. (21).

Solution Technique

Equations (6), (21), and (26), which may be solved simultaneously for T_e and T_v, given T, which is measured spectroscopically by TALIF or with CARS, are written as time dependent, and the steady-state solution is found by a relaxation

technique using the differential/algebraic equation solver LSODI.[24] The chemical rate terms are evaluated using the CHEMKIN (Ref. 25) subroutine package. Two calls to the rate of progress variable subroutine are made, one with the electron temperature in the calling argument when one of the reactants is an electron, and the other with the gas temperature in the calling argument when electrons are not reactants. This enables one to use the proper temperature that governs the reactions.

Results

Three cases have been investigated and results are presented here. The cases correspond to the situation in which the input microwave power and pressure in the reactor are varied while holding constant the size of the plasma ball in contact with the surface, in which case the ratio of power to total density P_{mw}/n is approximately constant. The plasma ball tends to grow with increasing power, whereas, it shrinks as the pressure increases. By adjusting these two parameters together, it is possible to hold the geometry (the radius R_p = 2.5 cm) of the plasma approximately fixed. The temperature of the substrate surface is held constant at 1173 K for these three cases as well. The vibrational temperature is only known for one of the sets of experimental conditions, corresponding to an averaged power density of 9 W/cm^3. The H-atom molar fraction was deduced from spectroscopic analysis of the plasma involving the method of actinometry, which has been validated and calibrated previously.[26] The error on this measurement is estimated to be about 20% for the highest power density used. The objective of the calculations is to determine the properties of the plasma, including the species mole fractions, vibrational temperature, and electron temperature and density using the thermochemical model described in this article. These can then be compared with the measurements.

The method for obtaining the electron temperature, vibrational temperature, and species mole fractions consists of solving the species balance Eqs. (21) simultaneously with the vibrational energy Eq. (26) and the electron energy Eq. (6). This set of differential equations is solved using the LSODI relaxation method.

To account for some deviations from the general form of the rate equations as utilized in the CHEMKIN package we must modify some of the rates as follows. First, in the solution of Eq. (21), the rate coefficient for the formation of H^- ions must be modified to account only for those H_2 molecules in vibrational states with $v \geq 4$. That is, the density of H_2 molecules must be multiplied by a factor f_v that represents the fraction of H_2 that is in states greater or equal to four:

$$f_v = \sum_{v=4}^{\infty} \exp\left(-\frac{v\theta_v}{T_v}\right) \Big/ \sum_{v=0}^{\infty} \exp\left(-\frac{v\theta_v}{T_v}\right)$$

where v is the vibrational quantum number, T_v is the vibrational temperature, and θ_v = 5987 K is the characteristic vibrational energy difference between states $v = 0$ and $v = 1$ for H_2. It is only necessary to sum over the first few terms since they decrease rapidly with v at low T_v. Second, the dissociative recombination reaction involving e and H_3^+ has two possible outcomes. Janev et al.[19] indicate that for T_e less than about 11,000 K the ratio of the reaction rates for producing 3H is about 2.5 times greater than for producing $H^* + H_2^*$. Above 11,000 K the ratio is inverted. Since the results indicate that T_e is near 17,000 K, the constant in the rate coefficient expression is given as 8×10^{17} for production of H^* and H_2^* and 3.2×10^{17} for the production of 3H.

We solved the full chemical model [Eq. (21)] with reactions and rates described in Table 2 and the energy exchange parameters given in Table 1 for the measurement conditions given in Table 3. In the energy exchange expression for dissociation of H_2 by electrons via the single states, we have used the energy exchange coefficients corresponding to the anharmonic oscillator (AHO) given in Table 1. The species boundary-layer

Table 3 Constants used for surface reactions in solution of kinetics equations

Surface temperature, T_w, 1000 K
Plasma radius, R_p, 2.5 cm
H-atom recombination coefficient, γ_H, 0.1
Ion recombination coefficient, γ_{ions}, 1.0
Boundary-layer thickness, δ_H, δ_{ions}, 1.3 cm

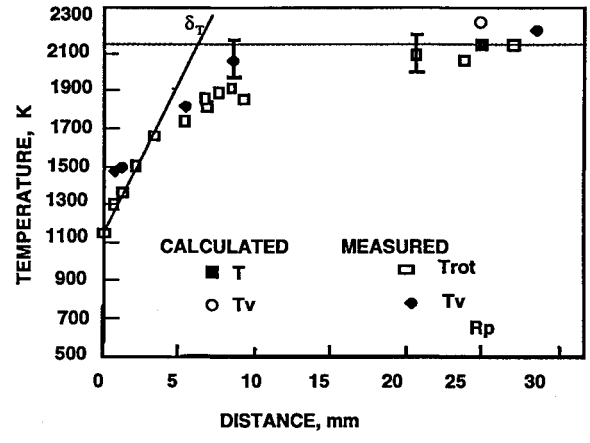

Fig. 6 CARS measured profiles of vibrational and rotational temperatures normal to surface in pure hydrogen plasma. Calculated T_v is shown along with T used in calculation at R_p = 25 mm. p = 2500 Pa, microwave power = 600 W, and flow rate = 300 sccm.

thickness δ for each species was assumed to be 1.3 cm as estimated from actinometry measurements using line intensities of H_α and Ar for case 1. This is almost two times thicker than that obtained from the CARS measurements of T_r seen in Fig. 6 denoted δ_T. The same value of δ was assumed for all cases based on a one-dimensional study of Hassouni,[26] which showed a very weak increase in boundary-layer thickness with pressure for the three cases of this study. The set of solutions for three cases is summarized in Table 4. We have found that T_e decreases from 17,800 to 16,800 K as the pressure and power increase together (at higher power density). As expected, T_v approaches T as the pressure increases. At 2500 Pa T_v is found to be 2256 K as shown in Fig. 6. This result agrees with the experimental trend that T_v is about 100–200 K greater than T, within experimental uncertainty. The electron density increases with pressure, whereas the electron mole fraction decreases. This is possibly because of the fact that H_2 dissociates significantly because of the increase of the gas temperature, while the electron temperature decreases somewhat. The decrease in electron temperature results from the greater electron energy loss at higher pressure. In our calculations we have held the boundary-layer thickness δ constant.

To assess the effect of species flux to the surface as accounted for by Eq. (22), we have parametrically varied δ from 0.7 to 1.6 cm for the three cases studied here. The results for the mole fractions of H_2 and electrons are given in Fig. 7. The calculated electron temperature and H-atom mole fraction are given in Fig. 8. We can see in these figures that the effect of the assumption of boundary-layer thickness is not large except for the dissociation fraction at the high-pressure–power case. The mole fraction of H tends to increase as the boundary layer is increased, especially for the high-pressure case. It is for this case that we have the greatest uncertainties and the greatest deviation of the results from actinometric measurements of the mole fraction of H atoms. Here, quenching is the largest and uncertainties in the quenching rates are most important. The other results, such as the calculated temperatures and species concentrations, are not largely affected.

In Table 4, comparing the mole fraction of H with that measured by actinometry[27] we see that the measured results agree

Table 4 Results of combined measured T with model equations

	Measured		
Case	1	2	3
P_{mw}, W	600	1,000	2,000
p, Pa	2,500	5,200	10,000
T, K	2,150	2,700	3,000
T_v, K	2,350		
Based on actinometry[27]			
X_H	0.04	0.083	0.32
Calculated from simultaneous solution of chemical rate and energy equations			
T_e, K	17,758	17,402	16,757
T_v, K	2,256	2,726	3,006
n_e, cm^{-3}	9.28E+11	1.04E+12	1.59E+12
X_{H_2}	0.946	0.925	0.788
X_H	0.054	0.075	0.212
X_{H^+}	5.7E-07	3.1E-07	7.6E-07
$X_{H_2^+}$	2.2E-09	1.9E-09	5.3E-09
$X_{H_3^+}$	1.1E-05	7.9E-06	6.1E-06
X_{H^-}	2.6E-07	7.4E-07	4.4E-07
Xe	1.1E-05	7.5E-06	6.4E-06
Calculated electron energy loss terms, W/m^3			
T_e, K	17,758	17,402	16,757
P_{mw}/V	9.17E+06	1.53E+07	3.06E+07
Q_{ev}	2.11E+06	3.71E+06	7.81E+06
Q_{te}	2.07E+06	3.66E+06	9.44E+06
Q_{ei}	8.13E+04	1.23E+05	2.28E+05
Q_{ed}^3	3.92E+06	6.25E+06	1.06E+07
Q_{ev}^{ie}	9.93E+05	1.54E+06	2.47E+06

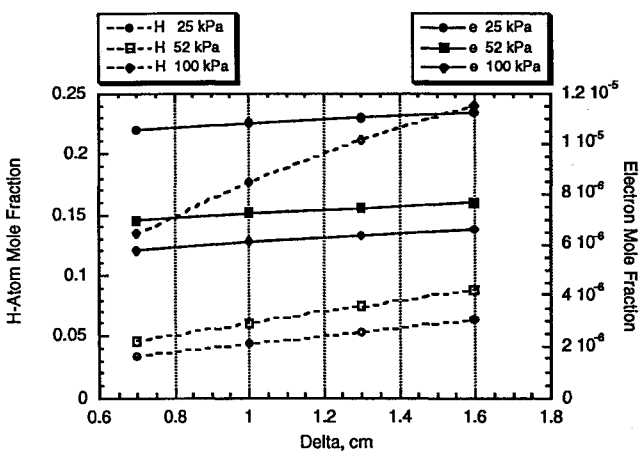

Fig. 7 Dependence of H-atom and electron mole fractions on species boundary-layer thickness.

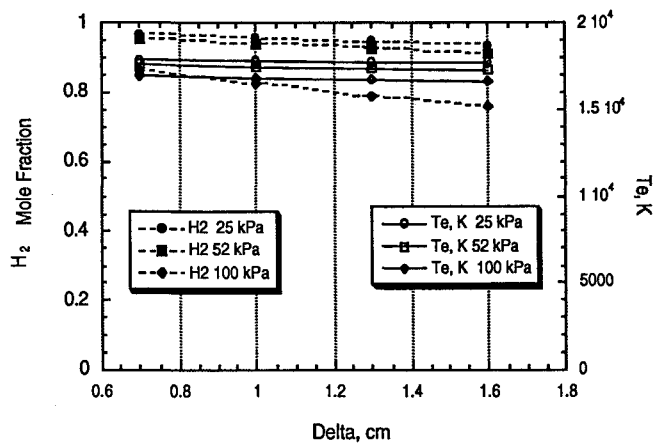

Fig. 8 Electron temperature and H_2 mole fraction dependence on assumed species boundary-layer thickness.

very well with the calculated results in cases 1 and 2. However, for the high-power case the agreement is not as good. The measured X_H is as low as 0.32.

In Table 4 we see that the electron fraction is on the order of 10^{-5} and that H_3^+ has the greatest mole fraction of the ions. Because of its role in dissociation and exchange reactions we expect H_2^+ to be an important species, even though it has the smallest mole fraction. H^+ and H^- are also minor species, but they too may be important in establishing the overall charge and energy balances. Quantifying this would require an investigation of the individual contributions to the rate equations and a sensitivity study that is outside the scope of this article.

The average power lost by the microwaves to heat the electrons was estimated from the power available and the volume of the visible plasma. It is interesting to assess which modes of electron energy loss are most influential in establishing the power balance in the plasma. The individual contributions to the losses are given in Table 4. We can see that H_2 has a major influence on the losses because the dominant loss term is dissociation of H_2 in all three cases. This is followed closely by electron–vibration exchange and electron–translation exchange. In the lower pressure cases these are about equal, however, at p = 10 kPa, Q_{te} is about 20% larger than Q_{ev}. We can also see that power loss via ionization is about a factor of 100 smaller than the total power absorbed. Ionization is important, however, to maintain charge balance.

Since the amount of power absorbed by the plasma is only estimated, a parametric study of the effect of absorbed power on the results was made by varying the net energy to the electrons from the microwave source. The results for the 2500-Pa case are shown in Fig. 9, where T_e and T_v are shown as functions of absorbed power. The total available power from the microwave generator was 600 W at this condition. The electron and H-atom mole fractions are shown in Fig. 10. Note that the actual amount of coupled power does not affect the temperatures significantly. The electron and H-atom mole fractions vary by about a factor of 2 to 3 over this range of absorbed power. Most likely, the electron fraction is more closely related to the H-atom fraction, as opposed to a sensitivity to T_e.

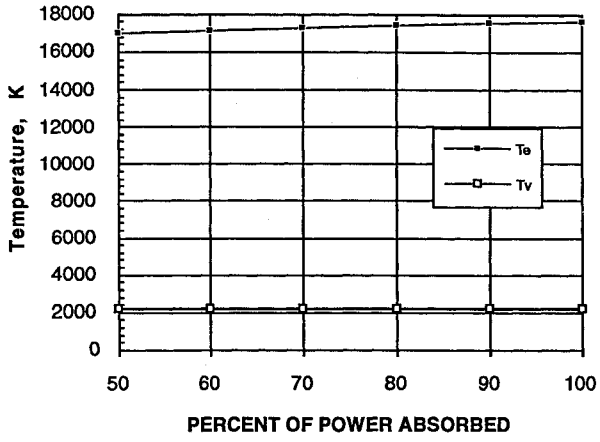

Fig. 9 Calculated variation of electron and vibrational temperature with power absorbed from microwave. P = 600 W and p = 2500 Pa.

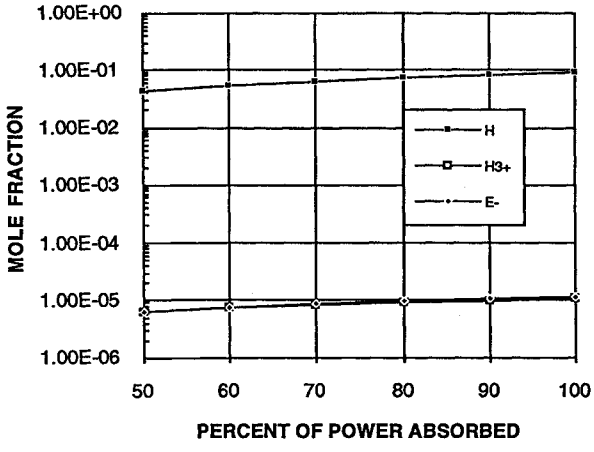

Fig. 10 Mole fractions of major ions with percent of absorbed microwave power. P = 600 W and p = 2500 Pa.

Concluding Remarks

A three-temperature model of a hydrogen plasma at moderate pressures has been proposed for use in calculating the properties of a microwave discharge used for developing diamond film deposition techniques. The model assumes thermal nonequilibrium between the rotational/translational, vibrational, and electron degrees of freedom, but it assumes that each degree of freedom can be described by a Maxwell/Boltzmann distribution at a given temperature. Twenty-seven chemical reactions are included. Fourteen of them depend on the electron temperature and one depends on the vibrational temperature as well as the electron temperature. The model is fashioned after that of Lee[10] for air at hypersonic flight conditions, but includes specific hydrogen reaction and excitation rates. Rate coefficients for vibration–electron coupling and dissociation and ionization of H_2 by electrons were determined using cross sections from the literature and assuming a Maxwellian EEDF. The rate of electron energy loss via excitation of the H_2 singlet states included the effect of vibrational excitation and was correlated with vibrational temperature.

Validation of the model must be based on its ability to predict measurements in the hydrogen microwave plasma. It was seen that, without actually solving the full multidimensional species and energy equations with heat conduction terms, it is possible to obtain an estimate of the electron temperature and density, as well as other properties, from a simultaneous solution of the chemical rate equations and the zero-dimensional vibrational and electron energy equations, given spectroscopic measurements of the rotational temperature. An estimate of the absorbed microwave power is required, but the results do not depend strongly on this parameter. Taking account of translation–vibration–electron energy coupling one can determine the consistency of the calculations with the measured vibrational temperature. At lower pressures the mole fractions of H_2 and H are in good agreement with those estimated from actinometry, but at 10 kPa the overall discrepancy in X_H is about 40–50%. The uncertainty in n_e is about a factor of 2, given that we have not included Maxwell's equations to determine the absorbed power.

We have seen that the H_2 molecules have a significant influence on energy electron energy exchange in the plasma and that the plasma is not highly dissociated at these conditions. We also have found that the major ion is H_3^+. Even though H^- and H_2^+ are very minor species, they may play a major role in the kinetics of the hydrogen microwave plasma.

The complete thermochemical model can be included in flow simulation calculations such as a finite difference solution of the Navier–Stokes equations; and as confidence is gained in the model and the computational methods for solving the pure hydrogen system, additional species will be added to permit one to account for deposition of carbon in the forms of graphite and diamond on substrates.

Acknowledgments

This work was supported in part by the Centre National de la Recherche Scientifique, DRET, and the Université Paris Nord. Discussions with Mario Capitelli and his pointing out and furnishing significant references have been invaluable. We gratefully acknowledge that Demetre Economou furnished his rate coefficients based on a non-Maxwellian EEDF for the comparisons included here.

References

[1]Scott, C. D., "A Nonequilibrium Model for a Moderate Pressure Hydrogen Microwave Discharge Plasma," NASA TM 104765, April 1993.

[2]Ferreira, C. M., and Moisan, M., "The Similarity Laws for the Maintenance Field and the Absorbed Power per Electron in Low-Pressure Surface Wave Produced Plasmas and Their Extension to HF Plasmas in General," *Physica Scripta*, Vol. 38, 1988, pp. 382–399.

[3]Gorse, C., Cacciatore, M., Celiberto, R., Cives, P., and Capitelli, M., *9th International Symposium on Plasma Chemistry* (Pugnochinso, Italy), edited by R. di'Agostino, Vol. 1, 1989, pp. 229–234.

[4]Gorse, C., Capitelli, M., Bacal, M., Bretagne, J., and Lagana, A., "Progress in the Non-Equilibrium Vibrational Kinetics of Hydrogen in Magnetic Multicusp H^- Ion Sources," *Chemical Physics*, Vol. 117, 1987, pp. 177–195.

[5]Loureiro, J., and Ferreira, C. M., "Electron and Vibrational Kinetics in the Hydrogen Positive Column," *Journal of Physics D: Applied Physics*, Vol. 22, 1989, pp. 1680–1691.

[6]Koemtzopoulos, C. R., Economou, D. J., and Pollard, R., "Hydrogen Dissociation in a Microwave Discharge for Diamond Deposition," *Diamond and Related Materials*, Vol. 2, 1993, pp. 25–35.

[7]Gicquel, A., Hassouni, K., Farhat, S., Breton, Y., Scott, C. D., Lefebvre, M., and Péalat, M., "Spectroscopic Analysis and Chemical Kinetics Modeling of a Diamond Deposition Plasma Reactor," *Diamond and Related Materials*, Vol. 3, 1994, pp. 581–586.

[8]Buckman, S. J., and Phelps, A. V., "Vibrational Excitation of D_2 by Low Energy Electrons," *Journal of Chemical Physics*, Vol. 82, No. 11, 1985, pp. 4999–5011.

[9]Buckman, S. J., and Phelps, A. V., "Tabulations of Collision Cross Sections and Calculated Transport and Reaction Coefficients for Electrons in H_2 and D_2," Univ. of Colorado, JILA Information Center Rept. 27, Boulder, CO, May 1985.

[10]Lee, J.-H., "Basic Governing Equations for the Flight Regimes of Aeroassisted Orbital Transfer Vehicles," *Thermal Design of Aeroassisted Orbital Transfer Vehicles*, edited by H. F. Nelson, Vol. 96, Progress in Astronautics and Aeronautics, AIAA, New York, 1985, pp. 3–53.

[11]Hiskes, J. R., "Cross Sections for the Vibrational Excitation of the $H_2X^1\Sigma_g^+(v)$ Levels Generated by Electron Collisional Excitation of the Higher Singlet States," *Journal of Applied Physics*, Vol. 70, No. 7, 1991, pp. 3409–3417.

[12]Cacciatore, M., Capitelli, M., and Dilonardo, M., "A Joint Vibro-Electronic Mechanism in the Dissociation of Molecular Hydrogen in

Nonequilibrium Plasmas," *Chemical Physics*, Vol. 34, 1978, pp. 193–204.

[13]Billing, G. D., and Fisher, V. V., "VV and VT Rate Coefficients in H_2 by a Quantum-Classical Model," *Chemical Physics*, Vol. 18, 1976, pp. 225–232.

[14]Audibert, M. M., Joffrin, C., and Ducuing, J., "Vibrational Relaxation of H_2 in the Range 500-40 K," *Chemical Physics Letters*, Vol. 25, March 1974, pp. 158–163.

[15]Millikan, R. C., and White, D. R., "Systematics of Vibrational Relaxation," *Journal of Chemical Physics*, Vol. 39, 1963, pp. 3209–3213.

[16]Kiefer, J. H., and Lutz, R. W., "Vibrational Relaxation of Hydrogen," *Journal of Chemical Physics*, Vol. 44, No. 2, 1966, pp. 668–672.

[17]Yos, J. M., "Transport Properties of Nitrogen, Hydrogen, Oxygen and Air to 30 000 K," Avco Corp., Research and Advance Development Div., RAD-TM-63-7, 1963.

[18]Curtiss, C. F., and Hirschfelder, J. O., "Transport Properties of Multicomponent Gas Mixtures," *Journal of Chemical Physics*, Vol. 17, No. 6, 1949, pp. 550–555.

[19]Janev, R. K., Langer, W. D., Evans, K., Jr., and Post, D. E., Jr., *Elementary Processes in Hydrogen-Helium Plasmas*, Springer–Verlag, Berlin, 1987.

[20]Drawin, H. W., and Emard, F., "Instantaneous Population Densities of the Excited Levels of Hydrogen Atoms and Hydrogen-Like Ions in Plasmas," *Physica C*, Vol. 85C, 1977, pp. 333–356.

[21]Massey, H. S. W., *Electronic and Ionic Impact Phenomena*, Vol. II, Electron Collisions with Molecules and Photoionization, Oxford, England, UK, 1969.

[22]Johnson, L. C., and Hinnov, E., "Ionization, Recombination, and Population of Excited Levels in Hydrogen Plasmas," *Journal of Quantitative Spectroscopy & Radiative Transfer*, Vol. 13, No. 4, 1973, pp. 333–358.

[23]Johnson, L. C., and Hinnov, E., "Rates of Electron-Impact Transitions between Excited States of Helium," *Physical Review*, Vol. 187, No. 1, 1969, pp. 143–152.

[24]Hindmarsh, A. C., "ODEPACK, a Systematized Collection of ODE Solvers, in Scientific Computing," edited by R. S. Stepleman, North-Holland, Amsterdam, 1983, pp. 55–64.

[25]Kee, R. J., Rupley, F. M., and Miller, J. A., "Chemkin-II: A Fortran Chemical Kinetics Package for the Analysis of Gas Phase Chemical Kinetics," Sandia National Labs. Rept. SAND89-8009B, Livermore, CA, April 1994.

[26]Hassouni, K., Farhat, S., and Scott, C. D., "Modeling of the Diffusional Transport of H_2 Plasma Obtained Under Diamond Deposition Discharge Condition," *Handbook of Industrial Diamonds and Diamond Films*, edited by M. Prelas, K. Bigelow, and G. Popovici, Marcel Dekker, New York, 1996, Chap. 7.1.

[27]Gicquel, A., Chenevier, M., and Lefebvre, M., "Modeling and Diagnostics of Plasma Reactors," *Handbook of Industrial Diamonds and Diamond Films*, edited by M. Prelas, K. Bigelow, and G. Popovici, Marcel Dekker, New York, 1996, Chap. 7.2.

[28]Takayanage, K., and Suzuki, H., *Cross Sections for Atomic Processes*, Vol. 1, Research Information Center, Inst. of Plasma Physics, Nagoya Univ., Chikusa-Ku, Nagoya, 464, Japan, Nov. 1978.

[29]Cohen, N., and Westburg, K. R., "Chemical Kinetic Data Sheets for High Temperature Chemical Reactions," *Journal of Physical and Chemical Reference Data*, Vol. 2, No. 3, 1983, pp. 531–564.

[30]Karpas, Z., Anicich, V., and Huntress, W. T., Jr., "An Ion Cyclotron Resonance Study of Ions with Hydrogen Atoms," *Journal of Chemical Physics*, Vol. 70, No. 6, 1979, pp. 2877–2881.

[31]Phelps, A. V., "Cross Sections and Swarm Coefficients for H^+, H_2^+, H_3^+, H, H_2, and H^- in H_2 for Energies from 0.1 eV to 10 keV," *Journal of Physical and Chemical Reference Data*, Vol. 19, No. 3, 1990, pp. 653–674.

[32]Raizer, Y. P., *Physics of Gas Discharge*, Nauka, Moscow, 1987.

[33]Matveyev, A. A., and Silakov, V. P., "Non-Equilibrium Kinetic Processes in Low-Temperature Hydrogen Plasma," Russian Academy of Sciences General Physics Inst., Preprint 8, IOFAN, Moscow, 1994.